

# FABRICATION AND CHARACTERIZATION OF LARGE-AREA FLEXIBLE CAPACITIVE MICROMACHINED ULTRASOUND TRANSDUCERS

Chloe Halbach<sup>1,2</sup>, Jeremy Segers<sup>1</sup>, Veronique Rochus<sup>1</sup>,  
Epimitheas Georgitzikis<sup>1</sup>, Paul Heremans<sup>1,2</sup> and David Cheyns<sup>1</sup>

<sup>1</sup>Imec, BELGIUM and <sup>2</sup>KU LEUVEN, BELGIUM

## ABSTRACT

Conventional Capacitive Micromachined Ultrasound Transducers (CMUTs) are generally produced on silicon wafers, limiting the size, form factor, hence applications, of the transducer arrays. In this paper, we unveil a CMUT fabrication technique that can enable the realization of high-density ultrasound arrays on large-area flexible substrates for a variety of new applications in ultrasonic sensing. We also compare optical inspection and electrical characterization methods to measure the pull-in voltage and resonance frequency of the fabricated CMUTs and show that these methods can be used to assess the yield and uniformity of the fabrication process.

## KEYWORDS

MEMS, flexible electronics, large area, polyimide, laser lift-off, ultrasonic sensor.

## INTRODUCTION

Commercially available ultrasound probes from Hitachi [1], Kolo Medical [2], and Butterfly Networks [3], and the more versatile Philips CMUT-on-CMOS technology platform previously demonstrated that CMUT-based ultrasound probes can compete with the bulk piezoelectric dominance in ultrasonic sensing. The primary advantages of CMUTs lie in their mass-manufacturing compatibility, direct integration capability with electronics, and miniaturization facility enabling the fabrication of high-density 2D-arrays with small pitch requirements. However, although the silicon wafer diameter is gradually increased to reduce cost in high-volume manufacturing, transducer arrays fabricated in silicon foundries rarely exceed 3 cm x 3 cm and will always be limited by the substrate size. The development of glass based CMUTs, compatible with flat panel display manufacturing [4], could overcome these restrictions in array size and pave the way towards transducer arrays with flexible form factors.

Some research groups have demonstrated the fabrication of CMUTs on glass wafers [5, 6], while others on a polyimide layer that can be released from a silicon carrier wafer by wet etching [7] or manual peeling [8]. In this paper, we report our progress towards the fabrication of CMUTs on a polyimide layer that can be released from a glass substrate by laser lift-off. The main advantage of this method is that it can be upscaled to panel size glass substrates and other types of sensors and imagers [9].

This paper comprises three main sections. First, we discuss the fabrication process and challenges. In this study, the CMUTs are manufactured by sacrificial release. Nevertheless, it is noteworthy to emphasize that low-temperature CMUT wafer bonding could also be compatible with the laser lift-off method. Secondly, measurements from a laser Doppler vibrometer, digital

holographic microscope, impedance analyzer and LCR meter are used to extract the CMUT resonance frequency and pull-in voltage. Ultimately, we show that electrical impedance measurements can be used to assess the yield and uniformity of the fabrication process at wafer level.

## FABRICATION

The CMUTs described in this paper have been processed on 6-inch Corning EAGLE XG borosilicate glass wafers. This type of glass is available in sizes up to Gen 10.5 (2.94 m x 3.37 m) and has been specifically designed for flat panel display industry. More specifically, its thermal expansion coefficient has been closely aligned with silicon to make it compatible with semiconductor-like processing. First, a high heat and chemically resistant U-Varnish-S polyimide (UBE) is spin coated and cured at 450 degrees Celsius to act as a flexible intermediate layer (12  $\mu$ m) between the glass wafer and the CMUT. This layer is used to delaminate the device from the glass carrier at the end of the fabrication process. Secondly, the CMUT stack is processed using a standard sacrificial release method. Finally, the flexible device can be released by laser lift-off from the glass carrier wafer and transferred to a curved substrate as illustrated in Figure 1.

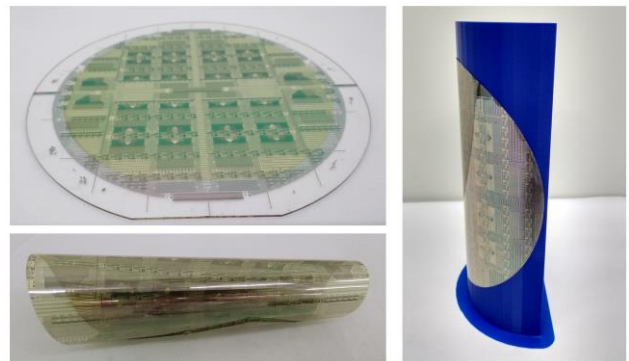


Figure 1: CMUTs on polyimide released by laser lift-off and transferred to a curved substrate with a radius of curvature of 4 cm.

## Sacrificial release process

A top view microscope image of a CMUT array is shown in Figure 2, while Figure 3 details the CMUT cross section immediately after sacrificial release. The Ti-Au-Ti bottom electrode (180 nm), the Cr sacrificial layer (100 nm), and the Ti-Au-Ti top electrode (250 nm) are patterned by lift-off. All these metal layers are evaporated to avoid protrusions. The Cr sacrificial layer is surrounded by 100 to 200 nm Inductively Coupled Plasma Chemical Vapor Deposition (ICPCVD) silicon nitride (SiN) to protect the electrodes from chromium etchant (Transene) during the 3.5-hour sacrificial release and to prevent electrical shorts during operation. Before sacrificial

release, the top electrode is covered with 500 nm ICPCVD SiN to make the first part of the membrane stiffer and to protect the top electrode. The Cr sacrificial layer is then reached by dry etching 3- $\mu\text{m}$  diameter release holes in the SiN membrane with  $\text{SF}_6/\text{O}_2$ . A critical point dryer (Automegasamdri-916B) is used immediately after sacrificial release to avoid capillary stiction and the release holes are subsequently filled with 500 nm ICPCVD SiN and 50 nm Atomic Layer Deposition (ALD) aluminum oxide ( $\text{Al}_2\text{O}_3$ ) to form a vacuum-sealed cavity. The latter deposition step is needed to fill the SiN stress lines through which water and air can penetrate. In summary, the CMUT membrane consists of 200 nm SiN, 250 nm Ti-Au-Ti, 1  $\mu\text{m}$  SiN, and 50 nm  $\text{Al}_2\text{O}_3$ . Ultimately, electrical contact pads are opened by dry etching  $\text{Al}_2\text{O}_3$  with  $\text{Cl}_2/\text{BCl}_3$  and SiN with  $\text{SF}_6/\text{O}_2$  to enable the CMUT electro-mechanical characterization.

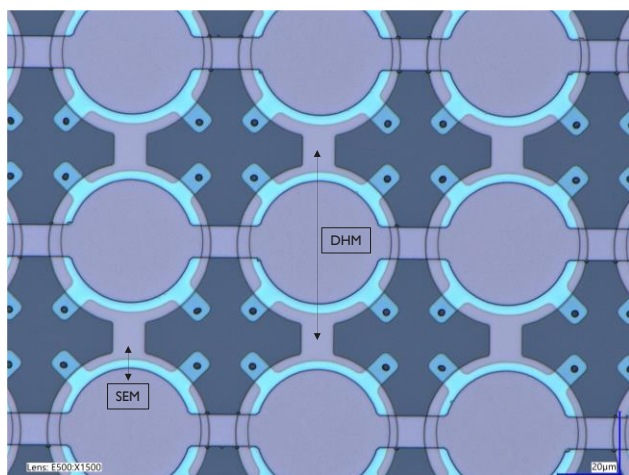


Figure 2: Top view microscope image of a CMUT array with a pitch of 64  $\mu\text{m}$  and release holes of 3  $\mu\text{m}$ . The arrows specify the locations used for the SEM cross section presented in Figure 3 and the membrane deflection displayed in Figure 4.

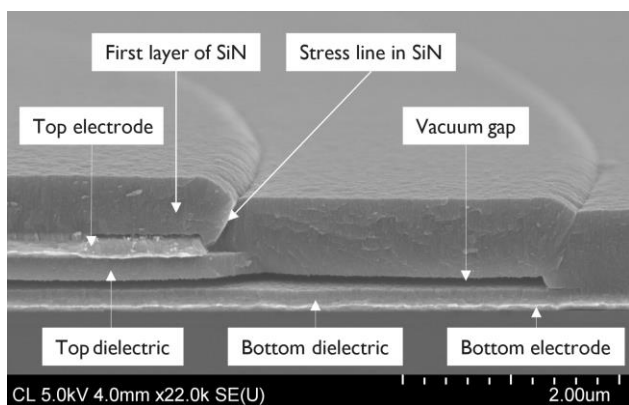


Figure 3: SEM cross section of the edge of a CMUT after sacrificial release but before via filling of the release holes.

### Laser lift-off

The main challenge in laser lift-off is to effectively separate the polyimide (PI) film from the glass substrate without deteriorating the device by the laser energy. Therefore, the fluence of the excimer laser debonder (ELD300) is optimized to avoid PI wrinkling and cracking of the functional layers, while ensuring a residue-free

removal process. Although Figure 1 shows that the PI foil is warping when it is wholly released from the glass substrate, it is possible to transfer the flexible device to another surface by pulling the outer edges of the film because warping does not occur directly after laser exposure.

## CHARACTERIZATION

Various characterization methods exist to measure the resonance frequency and pull-in voltage of CMUTs. Optical inspection methods are beneficial to study individual CMUT cell behaviors, whereas electrical methods are more effective to assess CMUT elements consisting of multiple cells. The initial membrane deflection, measured with a Digital Holographic Microscope (DHM, Lyncée Tec), is also a noteworthy measurement since it can strongly affect the resonance frequency and pull-in voltage. Figure 4 depicts the membrane profile of a CMUT with a cavity diameter of 42- $\mu\text{m}$  as a function of the applied DC voltage. The membrane center deflection of -90 nm at 0 V, resulting in a gap height of 20 nm, reveals considerable compressive residual stress that will reduce the resonance frequency and pull-in voltage compared to theoretical predictions for a membrane with zero initial deflection. Further optimization of the ICPCVD SiN deposition conditions (pressure, temperature,  $\text{SiH}_4$  and  $\text{N}_2$  gas flows) could reduce this effect. However, compressive residual stress leading to downwards membrane bending can be an advantage for collapse-mode operation since it strongly reduces the voltage needed to bring the membrane in collapse.

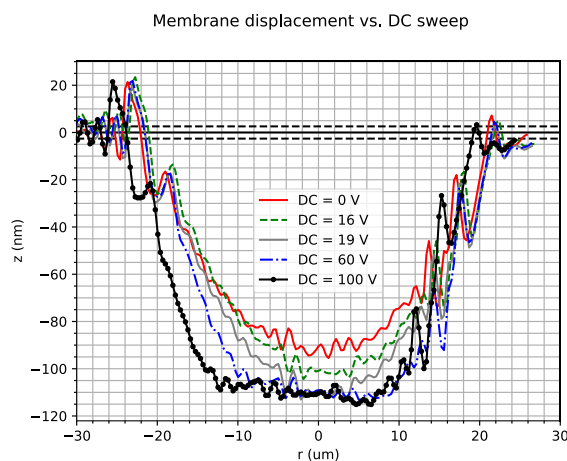


Figure 4: Membrane displacement ( $z$ ) of a 42- $\mu\text{m}$  diameter CMUT as a function of the radial position along the membrane ( $r$ ) and the applied DC voltage.

### Pull-in voltage

A first approach in measuring the pull-in voltage is to optically track the maximum membrane displacement as a function of the applied DC voltage with a DHM. Figure 4 reveals that the maximum membrane displacement of a 42- $\mu\text{m}$  diameter CMUT cell saturates at -110 nm when the DC bias exceeds 19 V. A second approach is to identify extrema in the capacitance-voltage or electrical impedance-voltage curves acquired with an LCR meter (Agilent E4980A) or impedance analyzer (Keysight

4294A), as shown in Figure 5. The AC voltage (0.5 V) is set at 100 kHz to avoid the CMUT resonance frequency, which is expected to be in the MHz range. The difference in capacitance (0.04 pF) measured by the LCR meter and impedance analyzer can be attributed to parasitic capacitance in the experimental setup (difference in wiring) but does not affect the pull-in identification as we seek a change in capacitance. The measurements were conducted on parallelly connected 3 x 3 CMUT cells of the same diameter as in Figure 4. Figure 5 shows an increase in capacitance (or decrease in impedance) with increasing DC bias due to the downwards movement of the membrane. When the membrane pulls in, the capacitance is expected to increase sharply. After pull-in, the capacitance continues to increase because the edges of the membrane are pushed down further with increasing DC bias. However, Figure 5 shows a drop in capacitance around pull-in. This counterintuitive drop can be ascribed to the dynamic membrane movement. The lack of appreciable changes in the real part and phase of the impedance compared to changes in the imaginary and absolute part of the impedance suggest that capacitive effects are dominating the change in electrical impedance. The drop in capacitance could be attributed to an upward motion of the membrane immediately after pull-in, here when the voltage exceeds 16 V. It can be shown with Comsol simulations that this phenomenon is only observed when the membrane exhibits a considerable initial deflection, resulting in a negligible sticking force at the center of the membrane if the voltage is ramped up slowly. Finally, it is noteworthy to mention that this drop in capacitance disappears with increasing AC voltage because the total applied voltage is ramped faster.

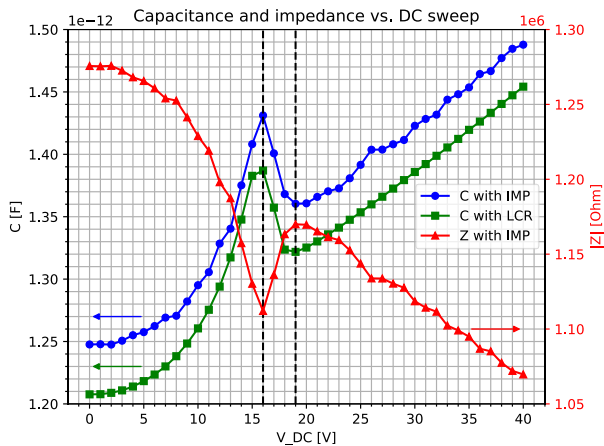


Figure 5: Capacitance  $C$  and electrical impedance  $Z$  of 3 x 3 CMUT cells with a membrane diameter of 42  $\mu\text{m}$  versus the applied DC voltage measured with an impedance analyzer (IMP) and an LCR meter. Pull-in occurs at 16 V, where a maximum in capacitance or minimum in impedance is observed.

One key difference between an LCR meter and an impedance analyzer is that the former is generally used at a fixed frequency, whereas the latter can perform frequency sweeps with a broader bandwidth. In the next section, we show that the Keysight 4294A impedance analyzer is also suitable to measure the CMUT resonance frequency.

## Resonance frequency

The mechanical resonance frequency of a CMUT is the frequency at which the membrane undergoes maximum deformation in response to an externally applied excitation, while the electrical resonance frequency is the frequency at which the capacitive reactance cancels out the inductive reactance, causing a minimum in the absolute value of the electrical impedance. To demonstrate the coupling between the electrical and mechanical resonances of a CMUT, we measured the membrane displacement and electrical impedance of a 38- $\mu\text{m}$  diameter membrane versus frequency ( $V_{AC} = 0.5 \text{ V}$ ) with a Laser Doppler Vibrometer (LDV, Polytec MSA-500) and the above-mentioned impedance analyzer. The results displayed in Figure 6 show an excellent correlation between the peak in the real part of the impedance, which coincides with a minimum in the absolute impedance, and the maximum in the normalized displacement from the LDV. Similar plots and matching resonance frequencies were obtained for DC biases below the collapse voltage. Displacement and impedance plots above the collapse voltage require further investigation since non-linear effects make it more difficult to identify the relation between the mechanical and electrical resonances.

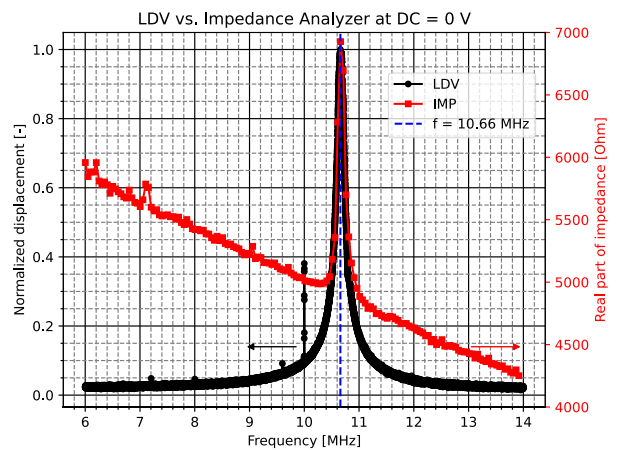


Figure 6: Membrane center displacement from a Laser Doppler Vibrometer (LDV) and real part of the electrical impedance from an impedance analyzer (IMP) as a function of the frequency sweep at zero DC bias for a membrane diameter of 38  $\mu\text{m}$ .

## Yield and uniformity

Optical measurement tools like digital holographic microscopes and laser Doppler vibrometers are indispensable to better understand the complex CMUT behavior and validate electro-mechanical coupling phenomena but are difficult to scale to large-area characterization because of their limited field of view, their sensitivity on wafer alignment and focal length, and the tremendous amount of data that would have to be processed per CMUT cell.

To illustrate the scalability of the electrical characterization methods, we connected the impedance analyzer to an automatic probe station and wrote a Python script that detects the pull-in voltage occurring at the local maximum of the capacitance. Similarly, we wrote a script that detects peaks in the real part of the impedance to

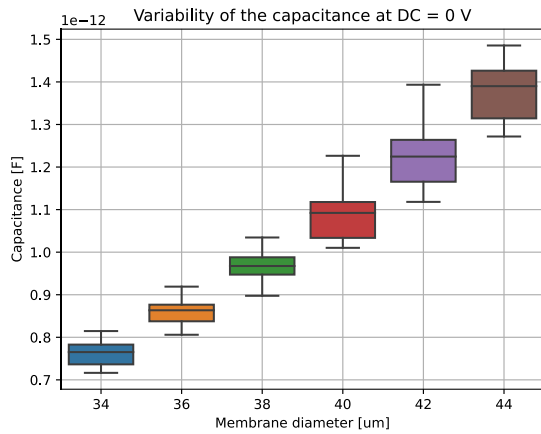


Figure 7: Capacitance deduced from electrical impedance measurements for 40 3x3 CMUT arrays.

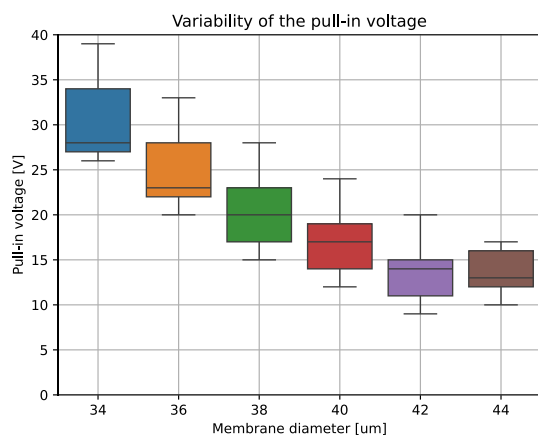


Figure 8: Pull-in voltage deduced from electrical impedance measurements for 40 3x3 CMUT arrays.

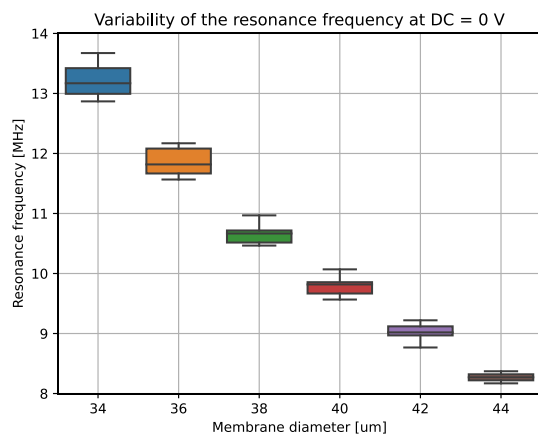


Figure 9: Resonance frequency deduced from electrical impedance measurements for 40 3x3 CMUT arrays.

extract the resonance frequency. The resonance frequencies are sorted by prominence when multiple peaks are detected so that they can be compared later with LDV. This is especially needed for collapsed CMUTs exhibiting important nonlinearities. A peak prominence threshold is used to filter out noisy data. Devices for which no peak is detected are listed as failed devices and used to compute the yield of the fabrication process. For example, an average pull-in detection ratio of 90 % is obtained for

membrane diameters ranging from 34 to 42  $\mu\text{m}$ , whereas the detection ratio of 44- $\mu\text{m}$  membrane diameters is only 62 % because some membranes were already collapsed after fabrication.

Figures 7, 8 and 9 show the variability in capacitance, pull-in voltage, and resonance frequency of 40 CMUT devices distributed across a 6-inch wafer. The relative variability in capacitance and pull-in voltage is greater than the relative variability in resonance frequency because the sacrificial layer is the layer with the greatest variability in film thickness (10-15 % for the Cr sacrificial layer, compared to 5 % for SiN). Variations in initial membrane deflection due to variations in residual stress can also show a strong impact on the variability of the measured parameters. Further studies are needed to define the acceptable variability range for ultrasound sensing.

## ACKNOWLEDGEMENTS

This work was funded by an SB PhD fellowship of the Research Foundation-Flanders [FWO, 1S27524N].

The authors would like to thank Tsung-Chieh Sun for his assistance in cleanroom processing, Clément Leruth for scanning electron microscopy (SEM), and François Berghmans for running the automatic prober.

## REFERENCES

- [1] T. Otake et al., “Development of 4G CMUT (CMUT Linear SML44 probe)” in *Advanced Ultrasound in Diagnosis and Therapy*, vol. 4, pp. 379-382, 2020.
- [2] D. Zhao et al., “A Commercialized High Frequency CMUT Probe for Medical Ultrasound Imaging”, *2015 IEEE IUS*, Taipei, October 21-24, 2015.
- [3] J. Rothberg et al., “Ultrasound-on-chip platform for medical imaging, analysis, and collective intelligence”, *Proc Natl Acad Sci USA*, July 6, 2021.
- [4] J. Souk et al., “Flat Panel Display Manufacturing”, *John Wiley & Sons*, 2018.
- [5] X. Zhang et al., “An optically transparent air-coupled capacitive micromachined ultrasonic transducer (CMUT) fabricated using adhesive bonding”, *2017 IEEE IUS*, Washington, September 6-9, 2017.
- [6] Adelegan et al., “Fabrication of 2D Capacitive Micromachined Ultrasonic Transducer (CMUT) Arrays on Insulating Substrates With Through-Wafer Interconnects Using Sacrificial Release Process” in *Journal of Microelectromechanical Systems*, vol. 29, no. 4, pp. 553-561, Aug. 2020.
- [7] Omidvar et al. “Flexible PolyCMUTs: Fabrication and Characterization of a Flexible Polymer-Based Capacitive Micromachined Ultrasonic Array for Conformal Ultrasonography” in *Advanced Material Technologies*, vol. 8, no. 5, pp. 2201316, March 2023.
- [8] I. Lucarini et al. “Demonstration of PolyimideBased Flexible CMUT Operation on Curved Substrates”, *2021 IEEE IUS*, Xi’an, September 11-16, 2021.
- [9] R. Delmdahl et al. “Large-Area Laser-Lift-Off Processing in Microelectronics” in *Physics Procedia*, vol. 41, pp. 241-248, 2013.

## CONTACT

\*Chloe Halbach, chloe.halbach@imec.be